Equation of Motion for the Solvent Polarization Apparent Charges in the Polarizable Continuum Model: Application to Real-Time TDDFT

Equation of Motion for the Solvent Polarization Apparent Charges in the Polarizable Continuum Model: Application to Real-Time TDDFT

Stefano Corni,*,† Silvio Pipolo,*,†,¶ and Roberto Cammi*,‡

Center S3, CNR Institute of Nanoscience, Modena, Italy, and Department of Chemistry, Università degli studi di Parma, Parma, Italy

E-mail: stefano.corni@nano.cnr.it; silvio.pipolo@nano.cnr.it; roberto.cammi@unipr.it

Abstract

When a solute charge density is evolving in time, e.g., due to an external perturbation, the solvent reaction field also becomes time-dependent, in a non-trivial way due to the delayed response of the solvent polarization rooted in its frequency-dependent dielectric constant. In Polarizable Continuum Models, the time-dependent reaction field is represented by time-dependent apparent surface charges. Here, we derive general expressions for such charges. In particular, for all the main flavors of PCM, including IEF-PCM, we show how the frequency-dependent dielectric function terms can be singled-out in diagonal matrices, most convenient for Fourier transforming. For spherical cavities such formulation highlights the relation with multipolar solvation models, and, when applied to the related context of metal nanoparticles, discloses a

*To whom correspondence should be addressed

†Center S3, CNR Institute of Nanoscience, Modena, Italy

‡Department of Chemistry, Università degli studi di Parma, Parma, Italy

¶Present affiliation: Ecole Normale Supérieure-PSL Research University, Dépt Chimie, Sorbonne Universités - UPMC Univ Paris 06, CNRS UMR 8640 PASTEUR, Paris, France

direct connection with multipolar plasmons. Using the Debye dielectric function, we derive a simple equation of motion for the apparent charges, free from system history. Such equation has been coupled to Real Time - Time Dependent Density Functional Theory (RT-TDDFT), to simulate the time evolution of the solute density rigorously accounting for the delayed solvent reaction field. The presented method seamlessly encompasses previous non-equilibrium approaches limited to an instantaneous solute potential change (e.g., a sudden electronic excitation), does not require additional assumptions beside the basic PCM's and it is not limited to iterative inversion procedures. Numerical examples are given, showing the importance of accounting for the delayed solvent-response effects.

1 Introduction

The dynamic behaviour of the composite system given by a molecule interacting with an external medium is better studied when the equation of motions of the entire system can be resolved into two, coupled equations of motion, one for the molecule and the other for the medium. This approach is particularly appealing to study the time-dependent phenomena of molecules in solution, where the time-dependence is not limited to the solute but it is also present for the solvent.[1] More complex systems, such as molecules interacting with nanoparticles[2] can also benefit from such approach.

When a molecular solute is in a non-stationary state, evolving in time according to the quantum-mechanics (QM) equation of motion (i.e. the time-dependent Schödinger equation), its charge density will be time-dependent, and the polarization induced in the solvent by such charge density will be also time-dependent. The time dependence of the solvent polarization is intrinsically complex: due to the presence of delayed components, the solvent polarization at a given time will be a function of the charge density at all the previous times. The main aim of this paper is to show how this complex time-evolution of the solvent polarization can be described by a suitable equation of motion, that should be consistently coupled with

the QM equation of motion of the molecular solute in order to give a coherent and detailed description of time-dependent phenomena of molecules in solution.

We consider the case of a molecule-solvent systems as described by the Polarizable Continuum Model (PCM) family of implicit solvation models,[3] descendants of the original Miertuš, Scrocco and Tomasi proposal.[4] The choice of focusing on PCM is related to the contributions that we have given in various times to its development, as well as to its current importance and widespread use. However, the relations which will be derived in this paper may be extended also to other implicit solvation models.[5–12] In PCM, a QM solute is hosted in a cavity of a dielectric medium representing the solvent and the polarization of the medium induced by the charged distribution of the solute is completely represented by apparent surface charges placed on the cavity boundary.

For time-dependent PCM problems, the responsive properties of the medium are characterized by the full spectrum of solvent frequency dependent dielectric permittivity $\epsilon(\omega)$,[13] and the basic equations relating the apparent surface charges to the charge distribution of the solvent are given in the frequency domain ω.[3,14–16] We remark that these basic relations are obtained from the equations for the time-*independent* PCM problem, by replacing in the PCM solvent response matrix the static dielectric permittivity with the frequency dependent permittivity.

Nowadays, PCM comprises a family of models, which differ in the representation of the PCM solvent response matrix and in the solute quantity entering the equations determining the apparent charges.[3] In this paper we will consider the frequency dependent PCM response matrices of all the main members of PCM: D-PCM,[4] IEF-PCM,[17,18] and C-PCM.[19] As a first result of this work, we show, for the first time, that it is possible to single-out the frequency dependent term of the PCM response matrix not only for the straightforward C-PCM case but also for D-PCM and for IEF-PCM. The frequency isolated form of the PCM matrices has many advantages. First, when it is applied to a spherical cavity it highlights a relation between the PCM and the multipole-expansion based solvation models.[5,6,12,20] Second, in

the case of the calculation of the optical properties of a spherical nanoparticle, it discloses a direct connection with multipolar plasmon resonances. However, the main advantage of the frequency isolated form lies in the derivation of PCM apparent charges in the time-domain.

Generally speaking, the apparent charges in the time-dependent PCM are obtained by the inverse Fourier transform of the frequency domain PCM charges.[21–26] We show that when the frequency isolated forms of the PCM matrices are used, it is possible to obtain a computational expression of the apparent charges in the time-domain which is able to treat an arbitrary time evolution of the charge density. This generalizes previous PCM approaches limited to (multi)-step evolution and approximated[24] or iterative[25,27] inversion procedures. The equations of motion for the polarization charges are finally obtained by taking the time derivative of the polarization charges expression as a function of time. Generally, these equations of motion are non Markovian and they are non local in time with respect to the time-dependent variation of the charge density. However, when the solvent dielectric is approximated as a Debye solvent[28] we could obtain a set of closed-form equations of motion for the polarization charges that depend on the solute charge density only at the given time.

Such equations of motion for the polarization charges of the solvent in the Debye approximation have been coupled with the real-time implementation of the PCM time-dependent density functional theory (PCM RT-TDDFT), and a numerical integration of the resulting system of equations has allowed following the time evolution of all the components of the solute-solvent system.

The present formulation generalizes our previous PCM RT-TDDFT method for the description of the interaction of a molecular solute with an external electromagnetic field.[29] With respect to other RT-TDDFT-PCM formulation for non-equilibrium solvation,[26,30] the present approach allows for a description of the polarization of the solvent with an arbitrary time-dependent evolution of the charge distribution of the molecular solute and contains no approximation besides the basic PCM's.

The paper is organized as follows: in section 2 we present the theoretical developments

that allow to write an equation of motion for the apparent charges and the computational implementation of the coupled PCM RT-TDDFT equations, then in section 3 we present numerical results that remark the importance of considering non-equilibrium effects and finally we draw the conclusions. The appendices contain the derivation that connects PCM to multipole-expansion for spherical cavities (appendix A) and a digression on the relation between the theory developed here and the plasmonic resonances of metal nanoparticles (appendix B).

2 Theory

The equations providing the apparent charges in the frequency domain $\mathbf{q}(\omega)$ are well known for all the PCM flavors considered here (C-PCM, IEF-PCM, D-PCM).[3] The general form is

$$\mathbf{q}(\omega) = \mathbf{Q}(\omega)\ \mathbf{g}(\omega) \tag{1}$$

where the matrix $\mathbf{Q}$ and the array $\mathbf{g}$ are given by:

C-PCM:

$$\begin{aligned} \mathbf{Q}^{\mathrm{CPCM}} &= f(\omega)\mathbf{S}^{-1} \\ f(\omega) &= -\frac{\epsilon(\omega)-1}{\epsilon(\omega)} \\ \mathbf{g}^{\mathrm{CPCM}} &= \mathbf{V}(\omega) \end{aligned} \tag{2}$$

IEF-PCM isotropic:

$$\begin{aligned} \mathbf{Q}^{\mathrm{IEF}} &= -\mathbf{S}^{-1}\left(2\pi\frac{\epsilon(\omega)+1}{\epsilon(\omega)-1}\mathbf{I}-\mathbf{DA}\right)^{-1}(2\pi\mathbf{I}-\mathbf{DA}) \\ \mathbf{g}^{\mathrm{IEF}} &= \mathbf{V}(\omega) \end{aligned} \tag{3}$$

D-PCM:

$$\begin{aligned} \mathbf{Q}^{\mathrm{DPCM}} &= -\left(2\pi\frac{\epsilon(\omega)+1}{\epsilon(\omega)-1}\mathbf{A}^{-1}-\mathbf{D}^{\dagger}\right)^{-1} \\ \mathbf{g}^{\mathrm{DPCM}} &= \mathbf{E_n}(\omega) \end{aligned} \tag{4}$$

Here, $\mathbf{A}$ is the diagonal matrix of the tesserae areas, $\mathbf{V}(\omega)$ contains the values of the frequency dependent potential generated by the oscillating molecular density at the positions of the tessera representative points $\vec{s}_i$, $\mathbf{E_n}(\omega)$ contains the components of the associated electric field normal to the cavity surface ($\vec{n}$) and the $\mathbf{S}$ and $\mathbf{D}$ matrix are defined in terms of $\vec{s}_i$:

$$D_{ij} = \frac{(\vec{s}_i - \vec{s}_j)\cdot\vec{n}_j}{|\vec{s}_i - \vec{s}_j|^3} \qquad S_{ij} = \frac{1}{|\vec{s}_i - \vec{s}_j|} \tag{5}$$

The charges in the time-domain, $\mathbf{q}(t)$, can be obtained by inverse Fourier transforming $\mathbf{q}(\omega)$. However, in their traditional forms recalled here above, only for C-PCM it is straightforwardly possible to single out the frequency dependent term and to perform the Fourier transform without having to numerically invert non-diagonal matrices at several frequencies.[31] In the first part of this section, we shall show how to rearrange IEF-PCM and D-PCM equations so to avoid such unfeasible numerical approach, without relying on approximations and iterative inversion procedures as done previously.[24,25] In the second part, we shall provide the expression of $\mathbf{q}(t)$ suitable for a generic frequency-dependent dielectric function $\epsilon(\omega)$; in the third part, an equation of motion for the charges in the case of a Debye dielectric function will be given, that is the most suitable to be coupled with RT-TDDFT. The details of this coupling are given in the last part of this section.

2.1 Singling-out the frequency dependence from the IEF-PCM and D-PCM matrices

The starting point is given by the IEF-PCM and D-PCM matrices reported as equations (3) and (4) above. Here we describe the details of the treatment for IEF-PCM only, as D-PCM follows a similar treatment, and for the latter only the final results will be given. Notably, up to a sign change in the definition of the matrix $\mathbf{D}$, the IEF-PCM equation is also the form used for investigating the optical properties of nanoparticles and of molecules close to nanoparticles,[2] so what follows applies also there.

From the IEF-PCM eq.(3), the vector of the frequency domain charges $\mathbf{q}(\omega)$ is given by:

$$\mathbf{q}(\omega) = -\left(2\pi\frac{\epsilon(\omega)+1}{\epsilon(\omega)-1}\mathbf{S} - \mathbf{DAS}\right)^{-1}(2\pi\mathbf{I} - \mathbf{DA})\,\mathbf{V}(\omega) \tag{6}$$

We now write $\mathbf{S} = \mathbf{S}^{1/2}\mathbf{S}^{1/2}$. This is possible as $\mathbf{S}$ is symmetric and positive defined. Then:

$$\mathbf{q}(\omega) = -\left(2\pi\frac{\epsilon(\omega)+1}{\epsilon(\omega)-1}\mathbf{S}^{1/2}\mathbf{S}^{1/2} - \mathbf{DAS}^{1/2}\mathbf{S}^{1/2}\right)^{-1}(2\pi\mathbf{I} - \mathbf{DA})\,\mathbf{V}(\omega) \tag{7}$$

and, collecting one $\mathbf{S}^{1/2}$ on the right and one on the left of the inverse matrix in eq. (7):

$$\begin{aligned}\mathbf{q}(\omega) = & -\mathbf{S}^{-1/2}\left(2\pi\frac{\epsilon(\omega)+1}{\epsilon(\omega)-1}\mathbf{I} - \mathbf{S}^{-1/2}\mathbf{DAS}^{1/2}\right)^{-1}\mathbf{S}^{-1/2} \\ & (2\pi\mathbf{I} - \mathbf{DA})\,\mathbf{V}(\omega)\end{aligned} \tag{8}$$

The matrix $\mathbf{S}^{-1/2}\mathbf{DAS}^{1/2}$ appearing in the above equation is symmetric, i.e., it is equal to its transpose $\mathbf{S}^{1/2}\mathbf{AD}^{\dagger}\mathbf{S}^{-1/2}$, as a consequence of the relation:[18]

$$\mathbf{DAS} = \mathbf{SAD}^{\dagger} \tag{9}$$

Therefore, such matrix is diagonalizable, i.e.,:

$$\mathbf{S}^{-1/2}\mathbf{DAS}^{1/2} = \mathbf{T}\mathbf{\Lambda}\mathbf{T}^{\dagger} \tag{10}$$

where $\mathbf{T}$ is the unitary matrix of the eigenvectors and $\mathbf{\Lambda}$ is the diagonal matrix of the real eigenvalues. Actually, in the computational practice, eq.(9) is only approximately valid and therefore $\mathbf{S}^{-1/2}\mathbf{DAS}^{1/2}$ is not exactly symmetric. In this work, the matrices $\mathbf{T}$ and $\mathbf{\Lambda}$ have been obtained by diagonalizing instead the symmetric matrix $1/2\left(\mathbf{S}^{-1/2}\mathbf{DAS}^{1/2} + \mathbf{S}^{1/2}\mathbf{AD}^{\dagger}\mathbf{S}^{-1/2}\right)$. Incidentally, this symmetrization is used in the implicit solvation method developed by Chipman.[8,9]

Now, by using the diagonal form eq.(10) in eq.(8) we get:

$$\mathbf{q}(\omega) \;=\; -\mathbf{S}^{-1/2}\mathbf{T}\left(2\pi\frac{\epsilon(\omega)+1}{\epsilon(\omega)-1}\mathbf{I} - \mathbf{\Lambda}\right)^{-1}\mathbf{T}^{\dagger}\mathbf{S}^{-1/2}\left(2\pi\mathbf{I} - \mathbf{DA}\right)\mathbf{V}(\omega) \tag{11}$$

We underline here that the above-presented procedure, i.e. the steps that allows to write eq.(11) starting from eq.(6) is an example of solution of a generalized eigenvalue problem[32] applied to the matrix $\mathbf{DAS}$. Moreover, to provide a parallelism with the Roothan-Hall equations,[32] we underline that the matrices $\mathbf{S}$ and $\mathbf{S^{-1/2}T}$ play respectively the role of the overlap matrix and the expansion coefficients matrix. Equation (11) can be further simplified by transforming also the remaining $\mathbf{D}$ matrix. Inserting $\mathbf{I} = \mathbf{S}^{1/2}\mathbf{S}^{-1/2}$ just after $\mathbf{DA}$ in eq. (11) and exploiting the same diagonalization as before, we arrive at:

$$\mathbf{q}(\omega) \;=\; -\mathbf{S}^{-1/2}\mathbf{T}\left(2\pi\frac{\epsilon(\omega)+1}{\epsilon(\omega)-1}\mathbf{I} - \mathbf{\Lambda}\right)^{-1}\left(2\pi\mathbf{I} - \mathbf{\Lambda}\right)\mathbf{T}^{\dagger}\mathbf{S}^{-1/2}\mathbf{V}(\omega) \tag{12}$$

Let us call $\mathbf{K}(\omega)$ the product of diagonal matrices appearing in this equation, i.e.:

$$\mathbf{K}(\omega) = \left(2\pi\frac{\epsilon(\omega)+1}{\epsilon(\omega)-1}\mathbf{I} - \mathbf{\Lambda}\right)^{-1}\left(2\pi\mathbf{I} - \mathbf{\Lambda}\right) \tag{13}$$

K is diagonal and its elements are readily obtained as:

$$K_{ii}(\omega) = \frac{2\pi - \Lambda_{ii}}{2\pi\frac{\epsilon(\omega)+1}{\epsilon(\omega)-1} - \Lambda_{ii}} \tag{14}$$

In the case of spherical cavities, the values of K_{ii} and their degeneracy have a clear connection with the multipolar expansion of the reaction field. Indeed, for a spherical cavity it is possible to demonstrate that the spherical harmonics Y_{lm} are eigenfunctions of the integral Calderon operators $\mathcal{S}$ and $\mathcal{D}$ (whose discretized representations are the matrices **SA** and **DA**, respectively), by spanning the Coulomb potential on spherical harmonics and using their orthogonality.[33] This is shown in appendix A, where we found that for a spherical cavity the eigenvalues Λ_{ii} and $K_{ii}(\omega)$ can be labeled with lm ($l = 0, 1...$ and $m = -l, ..., l$), have degeneracy $2l + 1$ and are given by:

$$\Lambda_{lm} = -\frac{2\pi}{2l+1} \tag{15}$$

$$K_{lm} = \frac{\epsilon(\omega) - 1}{\epsilon(\omega) + l/(l+1)} \tag{16}$$

In the lowest l elements of K_{lm}, one recognizes the dielectric constant-related standard factors of the Born ($l = 0$), Bell ($l = 1$) and Abraham ($l = 2$) models.[34] This result is quite relevant, as it creates a bridge between PCM and multipole expansion-based solvation models. In the numerical section we shall show to which level these relations are fulfilled numerically. The diagonalized IEF-PCM form is also useful when this method is applied to calculate optical properties of metal nanoparticles,[2] see appendix B.

When the diagonal matrix $\mathbf{K}(\omega)$ is introduced into eq. (12), we obtain:

$$\mathbf{q}(\omega) = -\mathbf{S}^{-1/2}\mathbf{T}\mathbf{K}(\omega)\mathbf{T}^{\dagger}\mathbf{S}^{-1/2}\mathbf{V}(\omega) \tag{17}$$

which defines a IEF-PCM matrix $\mathbf{Q}^{\mathrm{IEF(d)}}$:

$$\mathbf{Q}^{\mathrm{IEF(d)}} = -\mathbf{S}^{-1/2}\mathbf{T}\mathbf{K}(\omega)\mathbf{T}^{\dagger}\mathbf{S}^{-1/2} \tag{18}$$

where the superscript IEF(d) denotes the use of the diagonal matrix $\mathbf{K}(\omega)$ in building the response matrix.

The new form of the IEF-PCM matrix (18) has a definite numerical advantage in any situation where the response at several frequencies is required. In fact, once $\mathbf{S}^{1/2}$, $\mathbf{S}^{-1/2}$, $\mathbf{T}$ and $\mathbf{\Lambda}$ are obtained at the beginning of the calculations (requiring however two matrix diagonalizations), they can be used as are, changing only $\mathbf{K}(\omega)$. Thus, per each frequency of interest, one matrix inversion of the standard IEF-PCM is replaced by two matrix-times-vector multiplications. Also, it allows storing only the matrix $\mathbf{S}^{-1/2}\mathbf{T}$ and the diagonal matrix $\mathbf{\Lambda}$. However, the real advantage of this form is evident when the Fourier transform to the time domain is taken. This is the subject of the next section. Finally, we give here the corresponding expression for the D-PCM approach:

$$\begin{aligned} \mathbf{q}(\omega) &= -\mathbf{S}^{-1/2}\mathbf{T}\mathbf{K}^{\mathrm{DPCM}}\mathbf{T}^{\dagger}\mathbf{S}^{1/2}\mathbf{A}\mathbf{E}_{\mathbf{n}}(\omega) \\ K_{ii}^{\mathrm{DPCM}}(\omega) &= \frac{1}{2\pi\frac{\epsilon(\omega)+1}{\epsilon(\omega)-1} - \Lambda_{ii}} \\ K_{ij}^{\mathrm{DPCM}} &= 0 \quad i \neq j \end{aligned} \tag{19}$$

2.2 Time-dependent apparent charges as history-dependent quantities

The general expression for time-dependent charges can be promptly obtained by Fourier transform of eq.(2). For C-PCM and IEF-PCM (we omit D-PCM for its similarity with IEF-PCM) this leads to:

C-PCM:

$$\begin{aligned} \mathbf{q}(t) &= \int_{-\infty}^{\infty} dt' f(t-t') \mathbf{S}^{-1} \mathbf{V}(t') \\ f(t-t') &= \int_{-\infty}^{\infty} \frac{d\omega}{2\pi} e^{-i\omega(t-t')} f_D(\omega) \end{aligned} \tag{20}$$

IEF-PCM:

$$\begin{aligned} \mathbf{q}(t) &= -\int_{-\infty}^{\infty} dt' \ \mathbf{S}^{-1/2} \mathbf{T} \mathbf{K}(t-t') \mathbf{T}^{\dagger} \mathbf{S}^{-1/2} \mathbf{V}(t') \\ K_{ii}(t-t') &= \int_{-\infty}^{\infty} \frac{d\omega}{2\pi} e^{-i\omega(t-t')} K_{ii}(\omega) \\ K_{ij}(t-t') &= 0 \quad i \neq j \end{aligned} \tag{21}$$

In this form, both $f(t-t')$ for C-PCM and $\mathbf{K}(t-t')$ for IEF-PCM can be computed once for all at the beginning of the calculation for the given dielectric function $\epsilon(\omega)$ and then applied to any $\mathbf{V}(t')$. We remark that both time dependent kernels $f(t-t')$ and $\mathbf{K}(t-t')$ are 0 for $t' > t$, assuring that the causality principle is satisfied. This naturally results from the Fourier Transform of the corresponding frequency dependent quantities. We shall now explicitly derive the equation of motion for the PCM apparent charges for a specific, but very relevant, choice of a frequency dependent dielectric constant, i.e., Debye's:[28]

$$\epsilon(\omega) = \epsilon_d + \frac{\epsilon_0 - \epsilon_d}{1 - i\omega\tau_D} \tag{22}$$

where τ_D is the (transverse) dielectric relaxation time, ϵ_d is the dynamic dielectric constant and ϵ_0 the static dielectric constant. Note that the sign of ω in the denominator is determined by the convention used here for the Fourier transform.

Let us start the derivation for the case of C-PCM which allows various simplifications.

Within C-PCM, we have specifically

$$f_D(\omega) = -\frac{(\epsilon_d - 1)(1 - i\omega\tau_D) + \epsilon_0 - \epsilon_d}{\epsilon_d(1 - i\omega\tau_D) + \epsilon_0 - \epsilon_d} \tag{23}$$

and we also define the C-PCM function f and matrix $\mathbf{Q}^{\mathrm{CPCM}}$ for ϵ_d and ϵ_0:

$$f_d = -\frac{\epsilon_d - 1}{\epsilon_d}, \quad \mathbf{Q}_d^{\mathrm{CPCM}} = f_d \mathbf{S}^{-1} \tag{24}$$

$$f_0 = -\frac{\epsilon_0 - 1}{\epsilon_0}, \quad \mathbf{Q}_0^{\mathrm{CPCM}} = f_0 \mathbf{S}^{-1} \tag{25}$$

Performing the integral in eq.(20) and after some algebra, we end up with the following equation for the charges:

$$\begin{aligned} \mathbf{q}(t) &= \int_{-\infty}^{\infty} dt' \left[f_d \delta(t - t') + \frac{e^{-(t-t')/\tau_{\mathrm{CPCM}}}}{\tau_{\mathrm{CPCM}}} \Theta(t - t')(f_0 - f_d) \right] \mathbf{S}^{-1} \mathbf{V}(t') \\ &= \mathbf{Q}_d^{\mathrm{CPCM}} \mathbf{V}(t) + \int_{-\infty}^{\infty} dt' \frac{e^{-(t-t')/\tau_{\mathrm{CPCM}}}}{\tau_{\mathrm{CPCM}}} \Theta(t - t')(\mathbf{Q}_0^{\mathrm{CPCM}} - \mathbf{Q}_d^{\mathrm{CPCM}}) \mathbf{V}(t') \end{aligned} \tag{26}$$

where:

$$\tau_{\mathrm{CPCM}} = \tau_D \frac{\epsilon_d}{\epsilon_0} \tag{27}$$

is the relaxation time for C-PCM and turns out to be the longitudinal relaxation time of the dielectric and $\Theta(t - t')$ is the Heaviside step function. The latter ensures the correct causality condition[33] as stated above, i.e. only the values of the potential at times $t' \leq t$ contribute to determine the charges at time t. Equation (26) encompasses the evolution after a sudden change of the solute potential as a special case. In fact, let us suppose that the potential

$\mathbf{V}(t)$ has an abrupt jump at $t = 0$:

$$\begin{aligned} \mathbf{V}(t) &= \mathbf{V}_g \quad t < 0 \\ \mathbf{V}(t) &= \mathbf{V}_e \quad t \geq 0 \end{aligned} \tag{28}$$

where $\mathbf{V}_g$ may be the potential proper for the molecular ground state and $\mathbf{V}_e$ the potential for an excited state. Just after the jump (i.e., for $t = 0^+$) we get from eq.(26):

$$\mathbf{q}(0^+) \;=\; \mathbf{Q}_d^{\mathrm{CPCM}}\mathbf{V}_e + (\mathbf{Q}_0^{\mathrm{CPCM}} - \mathbf{Q}_d^{\mathrm{CPCM}})\mathbf{V}_g \tag{29}$$

that are the correct non-equilibrium apparent charges for the system. The inertial polarization then relaxes with constant τ_{CPCM}, reaching asymptotically the new equilibrium values $\mathbf{q} = \mathbf{Q}_0^{\mathrm{CPCM}}\mathbf{V}_e$ for $t \to \infty$.

For the diagonalized IEF-PCM, the procedure is very similar to that illustrated for C-PCM, although the algebra is more cumbersome. In particular, we end up with the following equations:

$$\mathbf{q}(t) \;=\; \mathbf{Q}_d^{\mathrm{IEF(d)}}\mathbf{V}(t) + \int_{-\infty}^{\infty} dt' \; \mathbf{Q}_{\mathrm{Deb}}^{\mathrm{IEF(d)}}(t - t')\mathbf{V}(t') \tag{30}$$

where $\mathbf{Q}_d^{\mathrm{IEF(d)}}$ is the $\mathbf{Q}_{\mathrm{Deb}}^{\mathrm{IEF(d)}}$ matrix defined in eq.(18) calculated for ϵ_d and $\mathbf{Q}_{\mathrm{Deb}}^{\mathrm{IEF(d)}}(t - t')$ is defined from eq.(18) in terms of a kernel diagonal matrix $\mathbf{K}_{\mathrm{Deb}}(t - t')$ whose elements are:

$$K_{\mathrm{Deb},ii}(t - t') = \frac{e^{-(t-t')/\tau_i}}{\tau_i}\Theta(t - t')(K_{0,ii} - K_{d,ii}) \tag{31}$$

$K_{0,ii}$ and $K_{d,ii}$ are built using ϵ_0 and ϵ_d, respectively, in eq.(14). At odds with C-PCM, the full IEF-PCM matrix has multiple relaxation times, which sounds reasonable since in a simpler Onsager-type model, each multipole has its own relaxation time. The expression of

τ_i is given in terms of the eigenvalues Λ_{ii}, defined before, as:

$$\tau_i = \tau_D \frac{(2\pi - \Lambda_{ii})\epsilon_d + 2\pi + \Lambda_{ii}}{(2\pi - \Lambda_{ii})\epsilon_0 + 2\pi + \Lambda_{ii}} \tag{32}$$

For a spherical cavity, based on the expression for Λ_{lm} in eq.(15), we get:

$$\tau_{lm} = \tau_D \frac{(l+1)\epsilon_d + l}{(l+1)\epsilon_0 + l} \tag{33}$$

Once more, as a function of l we obtain relaxation times related to the charge ($l = 0$, $\tau_{00} = \tau_D \epsilon_d/\epsilon_0$), dipole ($l = 1$, $\tau_{1m} = \tau_D(2\epsilon_d+1)/(2\epsilon_0+1)$, the Onsager model expression)[35–37] and higher multipoles.

2.3 Equation of motion of the time-dependent apparent charges for the Debye relaxation dielectric function

When the frequency dependence of the dielectric function is chosen to be Debye's (i.e., eq.(22)), it is possible to derive a differential equation for $\mathbf{q}(t)$ that is most suitable for implementation in a RT-TDDFT framework. We consider first the C-PCM model. Taking the derivative of eq.(26), we get:

$$\begin{aligned} \dot{\mathbf{q}}(t) &= \mathbf{Q}_d^{\mathrm{CPCM}} \dot{\mathbf{V}}(t) + \frac{1}{\tau_{\mathrm{CPCM}}} (\mathbf{Q}_0^{\mathrm{CPCM}} - \mathbf{Q}_d^{\mathrm{CPCM}}) \mathbf{V}(t) + \\ &\quad - \int_{-\infty}^{\infty} dt' \frac{e^{-(t-t')/\tau_{\mathrm{CPCM}}}}{\tau_{\mathrm{CPCM}}^2} \Theta(t-t') (\mathbf{Q}_0^{\mathrm{CPCM}} - \mathbf{Q}_d^{\mathrm{CPCM}}) \mathbf{V}(t') \end{aligned} \tag{34}$$

if we now rearrange eq.(26) as:

$$\int_{-\infty}^{\infty} dt' \frac{e^{-(t-t')/\tau_{\mathrm{CPCM}}}}{\tau_{\mathrm{CPCM}}} \Theta(t-t') (\mathbf{Q}_0^{\mathrm{CPCM}} - \mathbf{Q}_d^{\mathrm{CPCM}}) \mathbf{V}(t') = \mathbf{q}(t) - \mathbf{Q}_d^{\mathrm{CPCM}} \mathbf{V}(t) \tag{35}$$

and use it to replace the integral in eq.(34), we end up with a differential equation for the charges that reads:

$$\dot{\mathbf{q}}(t) = \mathbf{Q}_d^{\mathrm{CPCM}}\dot{\mathbf{V}}(t) + \frac{1}{\tau_{\mathrm{CPCM}}}\mathbf{Q}_0^{\mathrm{CPCM}}\mathbf{V}(t) - \frac{1}{\tau_{\mathrm{CPCM}}}\mathbf{q}(t) \tag{36}$$

This equation is very convenient for numerical implementation in the RT-TDDFT framework, as it does not require to store all the potentials at previous steps. Obviously, for static charges it reduces to the normal, time-independent, C-PCM equation.

For IEF-PCM (and D-PCM), it is also possible to write a differential equation for the apparent charges, since the evolution is just a linear superposition of exponential decays. The resulting equation is formally more complex:

$$\dot{\mathbf{q}}(t) = \mathbf{Q}_d^{\mathrm{IEF(d)}}\dot{\mathbf{V}}(t) + \tilde{\mathbf{Q}}\mathbf{V}(t) - \mathbf{R}\mathbf{q}(t) \tag{37}$$

where

$$\tilde{\mathbf{Q}} = -\mathbf{S}^{-1/2}\mathbf{T}\boldsymbol{\tau}^{-1}\mathbf{K}\mathbf{T}^{\dagger}\mathbf{S}^{-1/2} \tag{38}$$

$$\mathbf{R} = \mathbf{S}^{-1/2}\mathbf{T}\boldsymbol{\tau}^{-1}\mathbf{T}^{\dagger}\mathbf{S}^{1/2} \tag{39}$$

and $\boldsymbol{\tau}^{-1}$ is the diagonal matrix with elements $1/\tau_i$ defined in eq.(32).
It is straightforward to note that if we assume $\tau_i = \tau_{IEF}$ for each i, we get simpler, C-PCM like, equations for both the apparent charges and their derivatives:

$$\mathbf{q}(t) = \mathbf{Q}_d^{\mathrm{IEF(d)}}\mathbf{V}(t) + \int_{-\infty}^{\infty} dt' \frac{e^{-(t-t')/\tau_{\mathrm{IEF}}}}{\tau_{\mathrm{IEF}}}\Theta(t-t')\left(\mathbf{Q}_0^{\mathrm{IEF(d)}} - \mathbf{Q}_d^{\mathrm{IEF(d)}}\right)\mathbf{V}(t') \tag{40}$$

$$\dot{\mathbf{q}}(t) = \mathbf{Q}_d^{\mathrm{IEF(d)}}\dot{\mathbf{V}}(t) + \frac{1}{\tau_{\mathrm{IEF}}}\mathbf{Q}_0^{\mathrm{IEF(d)}}\mathbf{V}(t) - \frac{1}{\tau_{\mathrm{IEF}}}\mathbf{q} \tag{41}$$

How to choose the single relaxation time $\tau_{\rm IEF}$ is not unique. One possibility would be to choose the same relaxation time of the simpler C-PCM model, or the result for the Onsager model ($\tau_{\rm Ons} = \tau_D(2\epsilon_d+1)/(2\epsilon_0+1)$).[35–37] If a simple strategy to choose $\tau_{\rm IEF}$ is not at hand, the full equation should be used. It is to be remarked that to build $\mathbf{Q}_0$ and $\mathbf{Q}_d$ in eq.(41) there is no need to go through the diagonalization and the $\mathbf{K}$ matrix. They can be obtained as usual exploiting the standard IEF definition eq.(3), i.e., we can replace $\mathbf{Q}_0^{\rm IEF(d)}$ and $\mathbf{Q}_d^{\rm IEF(d)}$ by $\mathbf{Q}_0^{\rm IEF}$ and $\mathbf{Q}_d^{\rm IEF}$.

Finally, in view of the implementation in a RT-TDFT code that will be described in the next section, we note that besides the overhead for the initial matrices diagonalization (to be done once), there is no additional overhead for IEF-PCM (eq.(39)) with respect to C-PCM (eq.(34)) since, the required matrices are time independent and can be calculated once and for all at the beginning of the simulation.

2.4 Equation-of-motion time-dependent PCM

The general PCM non-equilibrium formalism presented in the previous section can be easily coupled with the standard RTTDDFT framework, as recently shown for an equilibrium approach[29] and as previously done for approximated non-equilibrium implementations.[26,30] We recall here that within such PCM-RTTDDFT formalism the time-dependent representation matrix of the Kohn-Sham PCM (KS-P) operator for the solvated system ($\mathbf{F}^{\mathbf{P}}_{\text{KS-P}}$) includes a solute-solvent interaction term ($\mathbf{V}^{\rm PCM}$), that represents the electrostatic potential operator generated by the time-dependent charges ($\mathbf{q}$):

$$\mathbf{F}^{\mathbf{P},\mathbf{q}}_{\text{KS-P}}(t) = \mathbf{F}^{\mathbf{P},0}_{\text{KS}} + \mathbf{V}^{\rm PCM}[\mathbf{q}(t)] - \vec{\boldsymbol{\mu}} \cdot \vec{E}_M(t) \tag{42}$$

here the dipole approximation in the length-gauge is used to express the radiation-matter interaction contribution in terms of the matrix associated to molecular dipole moment operator ($\vec{\boldsymbol{\mu}}$) and the time dependent Maxwell field ($\vec{E}_M(t)$); the cavity-field effects[29] are not

considered here for the sake of simplicity, but they can be included in terms of an effective molecular dipole moment.[38] The $\mathbf{F}^{\mathbf{P},0}_{\mathrm{KS}}$ term includes both the KS kinetic energy and potential operators and the dependence on the one-particle density matrix of the system ($\mathbf{P}$) is explicitly reported as apex to recall that this term implicitly depends on time as the density matrix is evolving. Atomic units are used throughout the entire article.

In line with the standard RT-TDDFT formalism,[39–41] the equations of motion for the PCM-RTTDDFT approach can be written in a convenient matrix form, once defined an orthonormal basis set, as follows:

$$[\mathbf{F}^{\mathbf{P},\mathbf{q}}_{\text{KS-P}}, \mathbf{P}] = i\dot{\mathbf{P}}(t) \tag{43}$$

Equation (43) can be then formally integrated to give:[42]

$$\mathbf{P}_{t+dt} = \mathbf{U}_{\mathbf{F}^{\mathbf{P},\mathbf{q}}_{\text{KS-P}}}\, \mathbf{P}_t\, \mathbf{U}^{\dagger}_{\mathbf{F}^{\mathbf{P},\mathbf{q}}_{\text{KS-P}}} \tag{44}$$

where $\mathbf{P}_t$ and $\mathbf{P}_{t+dt}$ are the density matrices at times t and $t+dt$ respectively, and $\mathbf{U}_{\mathbf{F}^{\mathbf{P},\mathbf{q}}_{\text{KS-P}}}$ is the representation matrix of the time propagator,[42] relative to the initial time t and the final time $t+dt$, expressed in terms of the representation matrix of the KS-P operator. A convenient formulation for the time propagator exploits the Magnus expansion[43] and the Gauss-Legendre quadrature[44] to provide a suitable form for increasing level of approximations. In this work we employ a second-order Magnus expansion (correct to $\mathrm{o}(dt^2)$),[42] to obtain the following working equation for the density matrix propagation:

$$\mathbf{P}_{t+dt} \simeq e^{-i\mathbf{F}^{\mathbf{P},\mathbf{q}}_{\text{KS-P}}(t+\frac{dt}{2})}\, \mathbf{P}_t\, e^{i\mathbf{F}^{\mathbf{P},\mathbf{q}}_{\text{KS-P}}(t+\frac{dt}{2})} \tag{45}$$

We use the *predictor-corrector* algorithm[42] to propagate the density matrix exploiting eq. (45) and a diagonal form of the $\mathbf{F}^{\mathbf{P},\mathbf{q}}_{\text{KS-P}}$ matrix to evaluate the propagator.[42,45] The orthonormal basis functions are defined from the standard atom-centered Gaussian basis set using

the Löwdin procedure.[32]

The *predictor-corrector* algorithm is a two-step strategy to propagate the density matrix at time $t + dt$ knowing $\mathbf{P}_t$. A first propagation (*predictor* step) to $t + \frac{dt}{2}$ is done to calculate $\mathbf{P}_{t+\frac{dt}{2}}$ needed to evaluate $\mathbf{F}^{\mathbf{P},\mathbf{q}}_{\text{KS-P}}(t + \frac{dt}{2})$. Such first propagation is performed using eq. (45) with a halved time-step ($dt' = \frac{dt}{2}$), and the density matrix ($\mathbf{P}_{t+\frac{dt'}{2}}$) needed to evaluate $\mathbf{F}^{\mathbf{P},\mathbf{q}}_{\text{KS-P}}(t + \frac{dt'}{2})$ is calculated from $\mathbf{P}_t$ using a linear extrapolation. Then, once built $\mathbf{F}^{\mathbf{P},\mathbf{q}}_{\text{KS-P}}(t + \frac{dt}{2})$, the propagation described in eq. (45) is performed (*corrector* step).

In parallel to the propagation of the density matrix (eq. (45)), a numerical solution to equations (36),(39) and (41) can be formulated by means of the Euler method,[46] obtaining respectively:

$$\mathbf{q}(t+dt) = \mathbf{Q}_d^{\text{CPCM}}[\mathbf{V}(t+dt) - \mathbf{V}(t)] + \frac{dt}{\tau_{\text{CPCM}}}\mathbf{Q}_0^{\text{CPCM}}\mathbf{V}(t) - \frac{dt}{\tau_{\text{CPCM}}}\mathbf{q}(t) + \mathbf{q}(t) \quad (46)$$

$$\mathbf{q}(t+dt) = \mathbf{Q}_d^{\text{IEF(d)}}[\mathbf{V}(t+dt) - \mathbf{V}(t)] + dt\tilde{\mathbf{Q}}\mathbf{V}(t) - dt\mathbf{R}\mathbf{q}(t) + \mathbf{q}(t) \quad (47)$$

$$\mathbf{q}(t+dt) = \mathbf{Q}_d^{\text{IEF}}[\mathbf{V}(t+dt) - \mathbf{V}(t)] + \frac{dt}{\tau_{\text{Ons}}}\mathbf{Q}_0^{\text{IEF}}\mathbf{V}(t) - \frac{dt}{\tau_{\text{Ons}}}\mathbf{q}(t) + \mathbf{q}(t) \quad (48)$$

Each of such equations, once coupled with the equation of propagation of the density matrix, defines one of the three different flavors of PCM-RTTDDFT scheme we use in this work, respectively denoted with the "CPCM", "IEF(d)" and "IEF τ_{Ons}" labels.

We underline that the mutual coupling between the classical evolution of the apparent charges ($\mathbf{q}$), and the quantum evolution of the density matrix ($\mathbf{P}$) is respectively mediated by the molecular potential $\mathbf{V}$ in eq.s (46)-(48), that obviously depends on the density matrix, and by the KS-PCM matrix $\mathbf{F}^{\mathbf{P},\mathbf{q}}_{\text{KS-P}}$ in eq. (45), which has a dependence on the apparent charges through the solute-solvent interaction term $\mathbf{V}^{\text{PCM}}[\mathbf{q}(t)]$.

The way we couple the propagation of the PCM charges $\mathbf{q}$ with the *predictor-corrector* algorithm is the following. Because the PCM charges are needed to evaluate the matrix $\mathbf{F}^{\mathbf{P},\mathbf{q}}_{\text{KS-P}}$, at times $t+\frac{dt'}{2}$ and $t+\frac{dt}{2}$, we start from the knowledge of the charges at the previous *corrector* propagation step, $\mathbf{q}(t - \frac{dt}{2})$, and we propagate them using a time-step $dt_{\mathbf{q}} = \frac{3}{4}dt$

for the current *predictor* step, and $dt_{\mathbf{q}} = dt$ for the current *corrector* step.

3 Computational application: Results and Discussion

In this numerical section, we first check the correctness and the numerical behavior of the implemented equations of motions for the PCM apparent charges. To this end, we analyze the case of a point-like unitary dipole "switched-on" at time $t = 0$ at the center of a spherical cavity embedded in a dielectric solvent.

We then apply the PCM-RTTDDFT combined propagation procedure described in section 2.4 to study the time dependence of the dipole moment of the helium atom and the lithium cyanide (LiCN) and methylcyclopropene (MCP) molecules, when a time-dependent electric field is acting on the system.

3.1 Computational details

Since our focus here is on solvent effects rather than the role of the xc functional, for the sake of implementation simplicity we limit our computational application to one local functional, BLYP.[47] In fact, non-local functionals require the use of complex (i.e., having both a real and an imaginary part) KS matrices in RT-TDDFT, making the implementation somewhat more involved. Anyway, there is no specific theoretical issue with such functionals in time-dependent PCM, and the approach we present in this work is also valid for them. All calculations are performed at the BLYP/cc-pVTZ[48] level of theory and the geometries of the LiCN and MCP molecules are optimized in solution using the IEF-PCM model. We used the static and dynamic dielectric constant of acetonitrile ($\epsilon_0 = 35.69$ $\epsilon_d = 1.807$). Considering that these are tests of the developed theory rather than a study on specific systems, we chose a computationally convenient τ_D of 2000 a.u. (48.38 fs). The simulations time-step is $dt = 0.2 a.u.$ (4.838 as). The diagonalization procedure of the $N \times N$ complex $\mathbf{F}^{\mathbf{P},\mathbf{q}}_{\text{KS-P}}$ matrix is performed by diagonalizing a $2N \times 2N$ real matrix, that is built from the

real and imaginary parts of the original $N \times N$ matrix (N = number of basis functions).[49] All calculations are performed with a locally modified version of the Gaussian G09 (A02) package.[50] To couple our PCM-RTTDDFT routine with the original Gaussian routines the $\mathbf{Q}_0$ and $\mathbf{Q}_d$ matrices are symmetrized and weights instead of charges are used to evaluate the $\mathbf{F}^{\mathbf{P},\mathbf{q}}_{\text{KS-P}}$ matrix.[51]

3.2 The sudden switching-on of a dipole in a spherical cavity

The numerical time-dependent reaction field along the dipole direction ($E^{\mathbf{q}}_R$), obtained from the time-dependent PCM charges (eqs. (46-48)) as follows

$$E^{\mathbf{q}}_R(t) = \sum_i q_i(t) \frac{\mathbf{r}_i \cdot \hat{\mathbf{r}}_{\mathbf{p}}}{|\mathbf{r}_i|^3} \tag{49}$$

is compared with the analytic solution for the Onsager spherical model,[35–37] which takes the following form:

$$E^{Ons}_R(t) = \frac{1}{R^3} \frac{2\epsilon_d - 2}{2\epsilon_d + 1} \left\{ 1 - \frac{3(\epsilon_0 - \epsilon_d)}{(2\epsilon_d - 2)(2\epsilon_0 + 1)} . \left[\exp\left(- \frac{t}{\tau_{Ons}} \right) - 1 \right] \right\} \tag{50}$$

Here $\mathbf{r}_i$ are the positions of the PCM charges, $\hat{\mathbf{r}}_{\mathbf{p}}$ is the unit vector defining the dipole moment direction, R is the cavity radius and the origin of the system of reference is placed at the center of the cavity. Such comparison is reported in Figure 1. A perfect agreement between the Onsager and the numerical profiles is found for both the IEF equations of propagation (eq.s (47)-(48)), i.e., both considering the entire IEF(d) equations or the simplified version with a single relaxation time chosen to be τ_{Ons}. The shape of the C-PCM profile is in line with the Onsager result, but the limit values at $t = 0$ and $t \to \infty$, are quantitatively different. In fact, we have seen before that the relaxation time in C-PCM is different from that in the Onsager expression, as well as the factors f_0 and f_d that determine the initial and final reaction fields. Nevertheless, differences are not large. A different f prefactor in the C-PCM equations (notably $f = -(\epsilon - 1)/(\epsilon + 1/2)$) would match the Onsager results

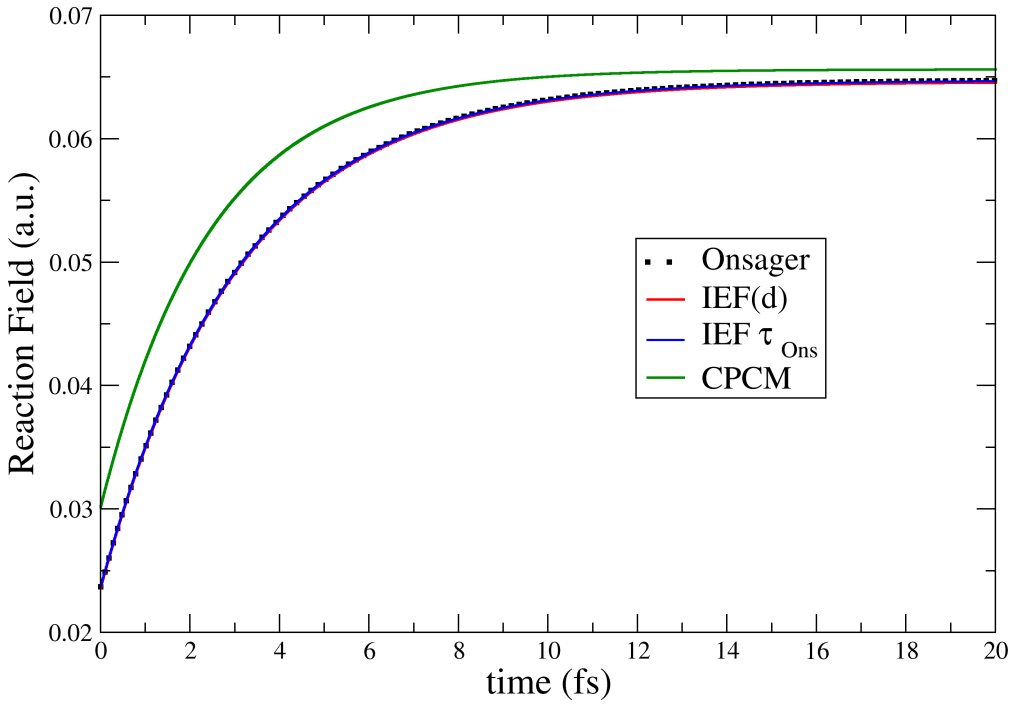

Figure 1: Reaction field profiles calculated with eq.s (49) (Onsager) and (50) in the case of point-like unitary dipole at the center of a spherical cavity embedded in a dielectric solvent. The labels "IEF(d)", "IEF τ_{Ons}" and "CPCM" refer to the coupling of eq. (50) with eq.s (47), (48) and (46) respectively.

quantitatively.

Table 1: Diagonal elements of the matrices $\mathbf{\Lambda}$, $\mathbf{K}$, $\mathbf{K}_d$ and $\boldsymbol{\tau}$, evaluated for the spherical cavity used in the calculation of the reaction field determined by a point-like dipole. A comparison with the theoretical values (Λ_{lm}, K_{lm} and τ_{lm}) reported in eq.s (15), (16) and (33) is performed. Because of the $2l+1$ degeneracy of the theoretical values only one of them is reported for each value of l. We limit this list to $i = 16$ and we recall that within this work $\tau_D = 48.38$ fs.

i	l	Λ_{ii}	Λ_{lm}	K_{ii}	K_{lm}	$K_{d,ii}$	$K_{d,lm}$	τ_{ii} (fs)	τ_{lm} (fs)
1	0	-6.2831	-6.2832	0.9720	0.9720	0.4466	0.4466	2.450	2.450
2	1	-2.0949	-2.0944	0.9586	0.9585	0.3498	0.3498	3.084	3.085
3		-2.0949		0.9586		0.3498		3.084	
4		-2.0949		0.9586		0.3498		3.084	
5	2	-1.2581	-1.2566	0.9542	0.9542	0.3262	0.3262	3.292	3.293
6		-1.2581		0.9542		0.3262		3.292	
7		-1.2581		0.9542		0.3262		3.292	
8		-1.2581		0.9542		0.3262		3.292	
9		-1.2581		0.9542		0.3262		3.292	
10	3	-0.9008	-0.8976	0.9520	0.9520	0.3157	0.3156	3.392	3.395
11		-0.9007		0.9520		0.3157		3.392	
12		-0.9007		0.9520		0.3157		3.392	
13		-0.9007		0.9520		0.3157		3.392	
14		-0.9004		0.9520		0.3157		3.392	
15		-0.9004		0.9520		0.3157		3.392	
16		-0.9004		0.9520		0.3157		3.392	

Next, we consider how well the real PCM quantities for a spherical cavity satisfy eq.s (15), (16) and (33). The first 16 diagonal elements of the matrices $\mathbf{\Lambda}$, $\mathbf{K}$, $\mathbf{K}_d$ and $\boldsymbol{\tau}$, evaluated for the spherical cavity, are reported in Table 1. The good agreement of the numerical results with equations (15)-(16), can be systematically improved by increasing the quality of the discretization of the surface (data not shown). We further underline here that, the diagonal elements of the $\mathbf{K}$ matrices correspond to the the reaction field factors (up to the cavity radius dependence) for the different terms determining the multipolar expansion of

the reaction field.[52]

3.3 PCM-RT-TDDFT simulations for He, LiCN and MCP

Let us now consider the results of PCM-RTTDDFT simulations. We use the following form for the applied electric field:

$$E(t) = \sum_{i}^{N_{\rm erf}} \frac{1}{2} E_i^{\rm max} \left[1 + {\rm erf}\left(\frac{t - t_i^c}{\sigma_i} \right) \right] \tag{51}$$

which is a convenient expression for a time-dependent profile that can be switched on and off in a smooth way. The amplitudes $E_i^{\rm max}$ can be both negative or positive, t_i^c and σ_i denote respectively the centers of the error functions and their widths. Concerning LiCN, the field is applied along the molecular symmetry axis, whereas for the MCP molecule the direction of the applied field is the one of the off-ring carbon-carbon bond. We have used two kinds of electric field profiles: a step-like and a sinusoidal-like profile generated using eq. (51) with two and five *erf* functions respectively.

In Figures 2 and 3 we report the time evolution of the dipole moment component along the applied field, with respect to its initial value ($\Delta\mu_E$), for the Helium atom and the LiCN and MCP molecules. The non-equilibrium effects are clearly stronger in the LiCN and MCP systems, as shown by the higher deviations of the "IEF τ_{Ons}" and "CPCM" profiles from the equilibrium one. This is reasonable, since in the case of LiCN and MCP the charges pre-existing the external electric field perturbations are different from 0, while for He they are initially null. For the electric field profile shown in Figure 2, the dipole clearly shows the effects of the delayed relaxation of the solvent polarization, both after the switching on of the field and after its switching-off. In the case of the sinusoidal-like electric field profile (Figure 3), non-equilibrium effects can instead be seen as a quenching of the field-induced dipole moment. In fact, the solvent reaction field is not able to adjust instantaneously to the solute charge density and the solute dipole is thus not maximized. To show that these

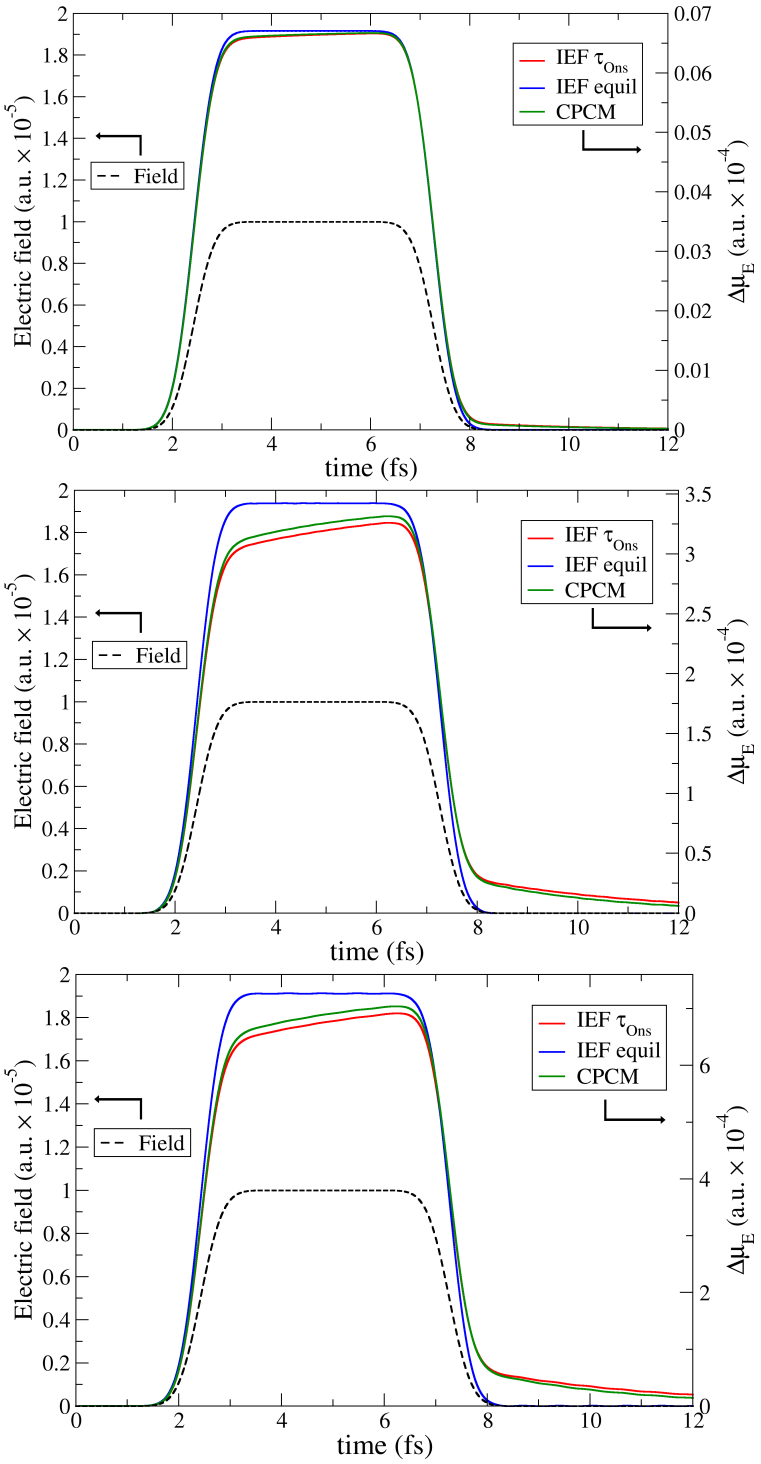

Figure 2: Dipole moment ($\Delta\mu_E$) profiles for He (fist row), LiCN (second row) and MCP (third row), obtained by propagating the density matrix with the combined non-equilibrium PCM-RTTDDFT scheme described in section 2.4. The labels "CPCM" and "IEF τ_{Ons}" refer to eq.s (46) and (48) respectively. The initial value is taken as zero. The IEF-PCM equilibrium value[29] ("IEF equil") is also reported for comparison. The electric field used is of the form described in eq. (51) with parameters $N_{\text{erf}} = 2$, $E_1^{\max} = -E_2^{\max} = 0.1$a.u., $t_1^c = 2.42$fs, $t_2^c = 7.26$fs, $\sigma_{1,2} = 0.484$fs.

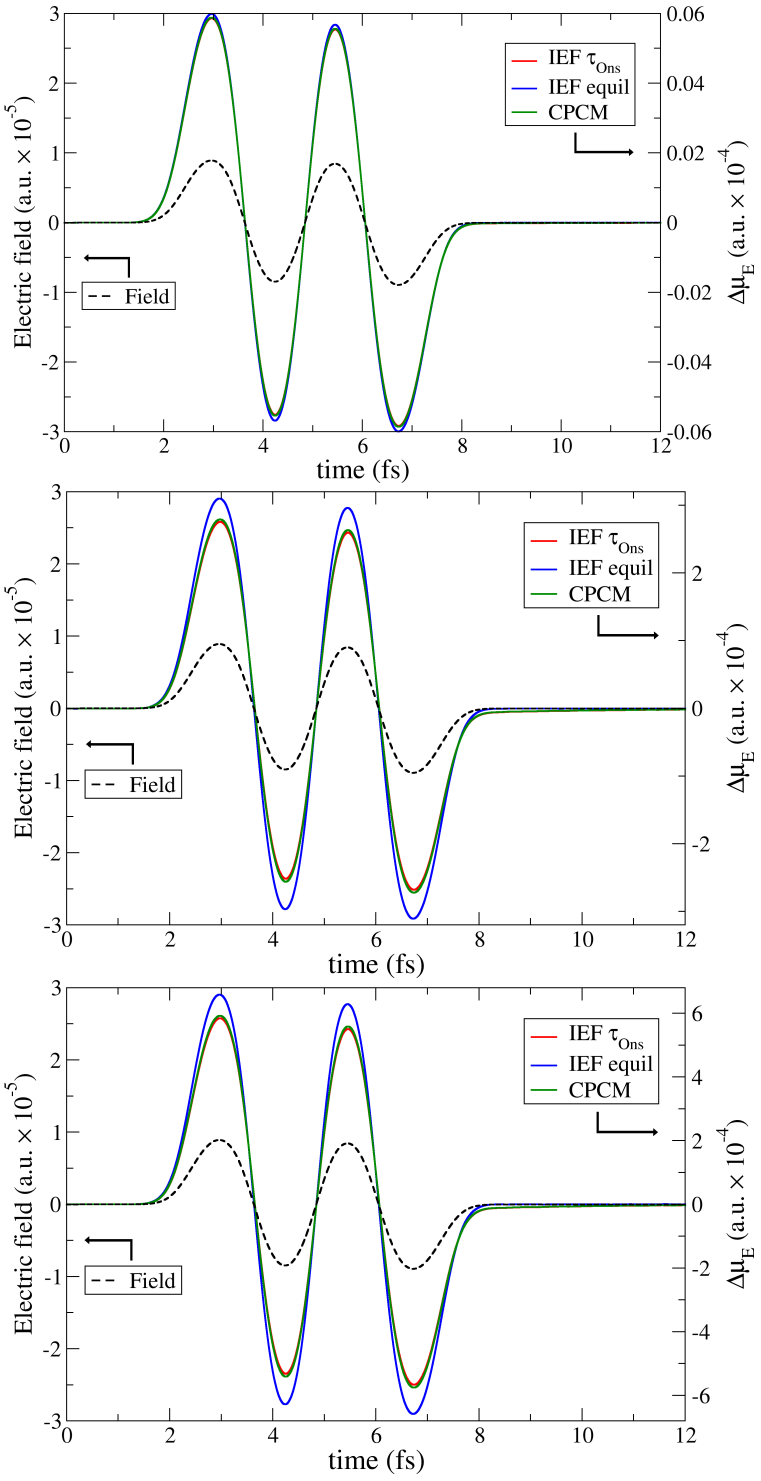

Figure 3: Dipole moment ($\Delta\mu_E$) profiles for He (fist row), LiCN (second row) and MCP (third row), obtained by propagating the density matrix with the combined non-equilibrium PCM-RTTDDFT scheme described in section 2.4. The labels "CPCM" and "IEF τ_{Ons}" refer to eq.s (46) and (48) respectively. The initial value is taken as zero. The IEF-PCM equilibrium value[29] ("IEF equil") is also reported for comparison. The electric field used is of the form described in eq. (51) with parameters $N_{\text{erf}} = 5$, $E_1^{\max} = -\frac{1}{2}E_2^{\max} = \frac{1}{2}E_3^{\max} = -\frac{1}{2}E_4^{\max} = E_5^{\max} = 0.1$a.u., $t_1^c = 2.42$fs, $t_2^c = 3.63$fs, $t_3^c = 4.84$fs, $t_4^c = 6.05$fs, $t_5^c = 7.26$fs, $\sigma_{1,5} = 0.484$fs.

effects are really due to the different time-behavior of the reaction field for the equilibrium and non-equilibrium case, we also report the reaction field profiles for He in Figure 4. Its behavior confirms the picture coming out from the dipole behavior, for both profiles of the applied electric field.

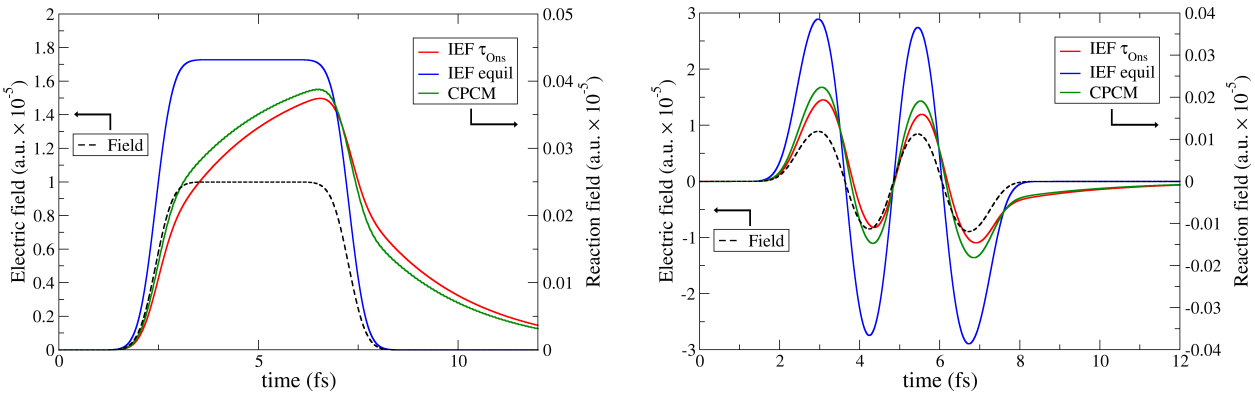

Figure 4: Reaction field profiles for He, obtained by propagating the density matrix with the combined non-equilibrium PCM-RTTDDFT scheme described in section 2.4. The labels "CPCM" and "IEF τ_{Ons}" refer to eq.s (46) and (48) respectively. The initial value is taken as zero. The IEF-PCM equilibrium value[29] ("IEF equil") is also reported for comparison. The electric fields used are of the form described in eq. (51) with parameters (i) $N_{\text{erf}} = 2$, $E_1^{\max} = -E_2^{\max} = 0.1$a.u., $t_1^c = 2.42$fs, $t_2^c = 7.26$fs, $\sigma_{1,2} = 0.484$fs (left) and (ii) $N_{\text{erf}} = 5$, $E_1^{\max} = -\frac{1}{2}E_2^{\max} = \frac{1}{2}E_3^{\max} = -\frac{1}{2}E_4^{\max} = E_5^{\max} = 0.1$a.u., $t_1^c = 2.42$fs, $t_2^c = 3.63$fs, $t_3^c = 4.84$fs, $t_4^c = 6.05$fs, $t_5^c = 7.26$fs, $\sigma_{1,5} = 0.484$fs (right).

4 Summary and Conclusions

With the present work we have provided a general method to treat non-equilibrium, time dependent solvation within the main versions of PCM (isotropic IEF, D-PCM and C-PCM). Such result has been achieved by providing an expression for the PCM apparent surface charges that account for the delayed polarization effects, due to the multiple-timescale relaxation of the solvent degrees of freedom. For IEF-PCM and D-PCM, a central role in this approach is played by a diagonal formulation of the corresponding matrices, that we have presented in section 2.1. It allows to single out the frequency-dependent dielectric-function terms and thus to avoid the Fourier transform of the entire, non-diagonal, PCM matrix, that would be computationally unfeasible. Furthermore, we have shown that such formulation discloses a direct connection between the PCM and multipole-based solvation models, linking, in the case of a spherical cavity, the eigenvalues of the PCM matrix with the factors of the multipolar expansion of the reaction field (section 2.1). Moreover, we have also performed a similar analysis on the IEF-PCM approach applied to spherical nanoparticles, that established a clear relation with multipolar plasmonic resonances. The diagonal PCM approach has been successfully tested, in section 3, against the Onsager analytical model for the reaction field within spherical cavities. The presented general approach does not require additional assumptions beside the basic PCM ones and it encloses previous non-equilibrium PCM formulations based on a sudden change of the solute wavefunction (such as an instantaneous electronic excitation) as special cases. Moreover, it is not limited to iterative inversion procedures.[25]

For generic frequency dependent dielectric functions, the expression of the time dependent apparent charges contains hystory-dependent terms, that make the numerical solution quite cumbersome. However, we have shown that in the important case of the Debye's dielectric function, it is possible to derive simple equations of motion for the apparent charges that do not involve the history of the system. Coupled to a recent PCM implementation of Real-Time TDDFT,[29] such differential equations lead to powerful working equations for solute density

propagation in solution, that rigorously account for the delayed solvent polarization (non-equilibrium effects). In perspective, the extension of such equation of motion to Debye's dielectric function with multiple relaxation times seems straightforward. For frequency-dependent dielectric functions tabulated at discrete frequencies (e.g., from experiments or molecular dynamics (MD) simulations), the definition of apparent charges in terms of a time integral given here can be used, although it is computational more cumbersome than the equation-of-motion approach. If the experimental or MD dielectric function can be fit to a sum of Debye terms, the strategy of using the proposed equations of motion with the parameters from the fitting is certainly more convenient.

The results obtained on test systems (He, LiCN and MCP - reported in section 3) by applying time-dependent electric fields with various profiles in time, show the significant difference between an equilibrium and a non-equilibrium solvation approach, highlighting the importance of taking into account such delayed solvent-response effects.

Here we have not considered local field effects, that are important for realistic spectroscopic applications.[29] As a future perspective, the non-equilibrium description of the solvent polarization presented in this work can be straightforwardly extended to the cavity-field treatment in PCM, where the solvent response is the one relative to the external field.

Acknowledgement

SC acknowledges funding from MIUR under the PRIN grant 2012A7LMS3_003. RC would like to thank Gaussian, Inc. for collaboration

A Deriving IEF(d) matrices for spherical cavities

In this section we show that spherical harmonics Y_{lm} are eigenfunctions of the Calderon integral operators $\mathcal{S}$ and $\mathcal{D}$, and thus that the diagonal matrices $\mathbf{\Lambda}$ and $\mathbf{K}$ have the elements given in eqs.(15) and (16). Let us start considering the action of $\mathcal{S}$ on $Y_{lm}(\theta, \phi)$ for a spherical cavity of radius R:

$$\mathcal{S} \cdot Y_{lm} = \int_S d\vec{s} \frac{1}{|\vec{s}\,' - \vec{s}|} Y_{lm}(\vec{s}) \tag{52}$$

where the integral is on the sphere surface. Replacing the Coulomb term with its expression in terms of spherical harmonics, and recalling that integrating on a sphere surface means to integrate on the spherical variables θ and ϕ:

$$\begin{aligned} \mathcal{S} \cdot Y_{lm} &= \sum_{l'=0}^{\infty} \sum_{m'=-l'}^{l'} R^2 \int_{-1}^{1} dcos\theta \int_0^{2\pi} d\phi \frac{4\pi}{2l'+1} \frac{s_<^{l'}}{s_>^{l'+1}} \\ & Y^*_{l'm'}(\theta, \phi) Y_{l'm'}(\theta', \phi') Y_{lm}(\theta, \phi) = \frac{4\pi R}{2l+1} Y_{lm}(\theta', \phi') \end{aligned} \tag{53}$$

For $\mathcal{D}$ the procedure is only slightly more complex. Recalling that for a spherical cavity $\hat{n} \cdot \vec{\nabla}$ is simply the derivative with respect to the radius in spherical coordinates, we have:

$$\mathcal{D} \cdot Y_{lm} = \int_S d\vec{s}\, Y_{lm}(\vec{s}) \hat{n}(\vec{s}) \cdot \vec{\nabla}_s \frac{1}{|\vec{s}\,' - \vec{s}|} = \frac{4\pi R^2}{2l+1} Y_{lm}(\theta', \phi') \frac{d}{ds} \left(\frac{s_<^l}{s_>^{l+1}} \right) \tag{54}$$

The last derivative has different values if calculated from the inside or from the outside of the cavity (from the inside, $s_< = s$, $s_> = s' = R$ thus it reads l/R^2; from the outside $s_< = s' = R$, $s_> = s$ thus it reads $-(l+1)/R^2$). This is due to the integration singularity that appears for $\vec{s} \to \vec{s}'$, that we have to cancel out. This can readily be accomplished taking the average of the derivative from the inside and from the outside, as the singularity

contributes the same term but with opposite signs to the two derivatives:

$$\mathcal{D} \cdot Y_{lm} = \frac{4\pi R^2}{2l+1} Y_{lm}(\theta', \phi') \frac{1}{2} \left(\frac{d}{ds}\bigg|_{in} \frac{s_<^l}{R^{l+1}} + \frac{d}{ds}\bigg|_{out} \frac{R_<^l}{s^{l+1}} \right) = -\frac{2\pi}{2l+1} Y_{lm}(\theta', \phi') \tag{55}$$

Using the matrix notation (and thus referring to numerically approximated identities):

$$\mathbf{SA}\ \mathbf{Y}_{lm} = \frac{4\pi R}{2l+1} \mathbf{Y}_{lm} \tag{56}$$

$$\mathbf{DA}\ \mathbf{Y}_{lm} = -\frac{2\pi}{2l+1} \mathbf{Y}_{lm} \tag{57}$$

which allow to demonstrate that $\mathbf{A}^{1/2}\mathbf{Y}_{lm}$ are the eigenvectors of the matrix $\mathbf{S}^{-1/2}\mathbf{DAS}^{1/2}$:

$$\mathbf{S}^{-1/2}\mathbf{DAS}^{1/2}\ \mathbf{A}^{1/2}\mathbf{Y}_{lm} = \mathbf{A}^{1/2}(\mathbf{SA})^{-1/2}\mathbf{DA}(\mathbf{SA})^{1/2}\mathbf{Y}_{lm} = -\frac{2\pi}{2l+1}\mathbf{A}^{1/2}\mathbf{Y}_{lm} \tag{58}$$

Since Λ_{ii} are the eigenvalues of this matrix by definition, eq.(15) follows.

B Plasmonic resonances of a nanoparticle by the IEF(d) approach

As mentioned in the main text, the matrix $\mathbf{Q}$ and $\mathbf{g}$ previously used to simulate optical absorption of complex shaped nanoparticles[2] are very similar to the IEF one, but for a sign change:

$$\begin{aligned} \mathbf{Q}^{\mathrm{NP}} &= -\mathbf{S}^{-1} \left(2\pi \frac{\epsilon(\omega)+1}{\epsilon(\omega)-1} \mathbf{I} + \mathbf{DA} \right)^{-1} (2\pi \mathbf{I} + \mathbf{DA}) \\ \mathbf{g}^{\mathrm{NP}} &= \mathbf{V}_{ex}(\omega) \end{aligned} \tag{59}$$

where $\mathbf{V}_{ex}(\omega)$ now represents the potential associated with an externally applied field. It is straightforward to exploit the same procedure used above for IEF to get the expression of the matrix $\mathbf{K}^{\mathrm{NP}}$:

$$K_{ii}^{\mathrm{NP}}(\omega) = \frac{2\pi + \Lambda_{ii}^{NP}}{2\pi\frac{\epsilon_M(\omega)+1}{\epsilon_M(\omega)-1} + \Lambda_{ii}^{NP}} \tag{60}$$

where ϵ_M is the metal dielectric function. Plasmon resonances can be recognize as maxima of the image part of the apparent charges as a function of frequency. In the form of eq.(60), this translates to frequencies that nullify the real part of the denominator; clearly each ii has its own plasmon frequency (up to symmetry related degeneracy). A similar analysis has been provided before.[53,54] For spherical nanoparticles, we can exploit the expression of Λ_{ii} in eq.(15) to find $K_{ii}^{\mathrm{NP,Sphe}}(\omega)$:

$$K_{lm}^{\mathrm{NP,Sphe}}(\omega) = \frac{\epsilon_M(\omega) - 1}{\epsilon_M(\omega) + (l+1)/l} \tag{61}$$

Nullifying the real part of the denominator in eq.(61) leads to the usual condition for the multipolar plasmons of the spherical particles. For example, the dipolar plasmon (the only excitable by radiation) has $l = 1$ which requires $\Re(\epsilon_M(\omega)) = -2$. For an arbitrarily shaped nanoparticle the geometric effects on the plasmon frequencies are all contained in $\Lambda_{ii}^{\mathrm{NP}}$: once such values have been determined, the plasmon frequencies of different materials can be calculated by solving $\Re\left(2\pi(\epsilon_M(\omega)+1)/(\epsilon_M(\omega)-1) + \Lambda_{ii}^{NP}\right) = 0$.

References

(1) Tomasi, J. In *Continuum Solvation Models in Chem. Phys.: From Theory to Applications*; Mennucci, B., Cammi, R., Eds.; Wiley & Sons: Chichester, UK, 2007; Chapter Sect. 1.1, p 16.

(2) Corni, S.; Tomasi, J. Enhanced Response Properties of a Chromophore Physisorbed on a Metal Particle. *J. Chem. Phys.* **2001**, *114*, 3739–3751.

(3) Tomasi, J.; Mennucci, B.; Cammi, R. Quantum Mechanical Continuum Solvation Models. *Chem. Rev.* **2005**, *105*, 2999–3093.

(4) Miertuš, S.; Scrocco, E.; Tomasi, J. Electrostatic Interaction of a Solute with a Continuum. A Direct Utilizaion of AB Initio Molecular Potentials for the Prevision of Solvent Effects. *Chem. Phys.* **1981**, *55*, 117–129.

(5) Rivail, J.-L.; Rinaldi, D. A Quantum Chemical Approach to Dielectric Solvent Effects in Molecular Liquids. *Chem. Phys.* **1976**, *18*, 233–242.

(6) Mikkelsen, K. V.; Agren, H.; Jensen, H. J. A.; Helgaker, T. A Multiconfigurational Self-Consistent Reaction-Field Method. *J. Chem. Phys.* **1988**, *89*, 3086–3095.

(7) Klamt, A. Conductor-Like Screening Model for Real Solvents: A New Approach to the Quantitative Calculation of Solvation Phenomena. *J. Phys. Chem.* **1995**, *99*, 2224–2235.

(8) Chipman, D. M. Charge Penetration in Dielectric Models of Solvation. *J. Chem. Phys.* **1997**, *106*, 10194–10206.

(9) Chipman, D. M. Reaction Field Treatment of Charge Penetration. *J. Chem. Phys.* **2000**, *112*, 5558–5565.

(10) Cramer, C. J.; Truhlar, D. G. Implicit Solvation Models: Equilibria, Structure, Spectra, and Dynamics. *Chem. Rev.* **1999**, *99*, 2161–2200.

(11) Cramer, C. J.; Truhlar, D. G. A Universal Approach to Solvation Modeling. *Acc. Chem. Res.* **2008**, *41*, 760–768.

(12) Lipparini, F.; Stamm, B.; Cancès, E.; Maday, Y.; Mennucci, B. Fast Domain Decomposition Algorithm for Continuum Solvation Models: Energy and First Derivatives. *J. Chem. Theor. Comp.* **2013**, *9*, 3637–3648.

(13) Hsu, C.-P.; Song, X.; Marcus, R. A. Time-Dependent Stokes Shift and Its Calculation from Solvent Dielectric Dispersion Data. *J. Phys. Chem. B* **1997**, *101*, 2546–2551.

(14) Cammi, R.; Cossi, M.; Mennucci, B.; Tomasi, J. Analytical Hartree-Fock Calculation of the Dynamical Polarizabilities α, β, and γ of Molecules in Solution. *J. Chem. Phys.* **1996**, *105*, 10556–10564.

(15) Cammi, R.; Mennucci, B.; Tomasi, J. On the Calculation of Local Field Factors for Microscopic Static Hyperpolarizabilities of Molecules in Solution with the Aid of Quantum-Mechanical Methods. *J. Phys. Chem. A* **1998**, *102*, 870–875.

(16) Tomasi, J.; Cammi, R.; Mennucci, B.; Cappelli, C.; Corni, S. Molecular Properties in Solution Described with a Continuum Solvation Model. *PCCP* **2002**, *4*, 5697–5712.

(17) Mennucci, B.; Cances, E.; Tomasi, J. Evaluation of Solvent Effects in Isotropic and Anisotropic Dielectrics and in Ionic Solutions with a Unified Integral Equation Method: Theoretical Bases, Computational Implementation, and Numerical Applications. *J. Phys. Chem. A* **1997**, *101*, 10506–10517.

(18) Cancés, E.; Mennucci, B.; Tomasi, J. A New Integral Equation Formalism for the Polarizable Continuum Model: Theoretical Background and Applications to Isotropic and Anisotropic Dielectrics. *J. Chem. Phys.* **1997**, *107*, 3032–3041.

(19) Barone, V.; Cossi, M. Quantum Calculation of Molecular Energies and Energy Gradi-

ents in Solution by a Conductor Solvent Model. *J. Phys. Chem. A* **1998**, *102*, 1995–2001.

(20) Onsager, L. Electric Moments of Molecules in Liquids. *JACS* **1936**, *58*, 1486–1493.

(21) Basilevsky, M. V.; Parsons, D. F.; Vener, M. V. An Advanced Dielectric Continuum Approach for Treating Solvation Effects: Time Correlation Functions. I. Local Treatment. *J. Chem. Phys.* **1998**, *108*, 1103–1114.

(22) Parsons, D. F.; Vener, M. V.; Basilevsky, M. V. Advanced Continuum Approaches for Treating Time Correlation Functions. The Role of Solute Shape and Solvent Structure. *J. Phys. Chem. A* **1999**, *103*, 1171–1178.

(23) Song, X.; Chandler, D. Dielectric Solvation Dynamics of Molecules of Arbitrary Shape and Charge Distribution. *J. Chem. Phys.* **1998**, *108*, 2594–2600.

(24) Ingrosso, F.; Mennucci, B.; Tomasi, J. Quantum Mechanical Calculations Coupled with a Dynamical Continuum Model for the Description of Dielectric Relaxation: Time Dependent Stokes Shift of Coumarin C153 in Polar Solvents. *J. Mol. Liq.* **2003**, *3*, 21–46.

(25) Caricato, M.; Ingrosso, F.; Mennucci, B.; Tomasi, J. A Time-Dependent Polarizable Continuum Model: Theory and Application. *J. Chem. Phys.* **2005**, *122*, 154501–154512.

(26) Nguyen, P. D.; Ding, F.; Fischer, S. a.; Liang, W.; Li, X. Solvated First-Principles Excited-State Charge-Transfer Dynamics with Time-Dependent Polarizable Continuum Model and Solvent Dielectric Relaxation. *J. Phys. Chem. Letters* **2012**, *3*, 2898–2904.

(27) Caricato, M.; Mennucci, B.; Tomasi, J.; Ingrosso, F.; Cammi, R.; Corni, S.; Scalmani, G. Formation and Relaxation of Excited States in Solution: A New Time Dependent Polarizable Continuum Model Based on Time Dependent Density Functional Theory. *J. Chem. Phys.* **2006**, *124*, 124520–124533.

(28) Bottcher, C.; Bordewijk, P. *Theory of Electric Polarization, Vol. 2*; Elsevier Science: Amsterdam, 1978.

(29) Pipolo, S.; Corni, S.; Cammi, R. The Cavity Electromagnetic Field Within the Polarizable Continuum Model of Solvation: An Application to the Real-Time Time Dependent Density Functional Theory. *Comput. Theor. Chem.* **2014**, *1040–1041*, 112–119.

(30) Liang, W.; Chapman, C. T.; Ding, F.; Li, X. Modeling Ultrafast Solvated Electronic Dynamics Using Time-Dependent Density Functional Theory and Polarizable Continuum Model. *J. Phys. Chem.. A* **2012**, *116*, 1884–90.

(31) Cammi, R. *unpublished*

(32) Szabo, A.; Ostlund, N. S. *Modern Quantum Chemistry: Introduction to Advanced Electronic Structure Theory*; DoverPublications. com, 1989.

(33) Jackson, J. D. *Classical Electrodynamics*, 3rd ed.; John Wiley & Sons: New York, 1999.

(34) Tomasi, J.; Persico, M. Molecular Interactions in Solution: An Overview of Methods Based on Continuous Distributions of the Solvent. *Chem. Rev.* **1994**, 2027–2094.

(35) van Gunsteren, W. F.; Berendsen, H. J. C.; Rullmann, J. A. C. Inclusion of Reaction Fields in Molecular Dynamics : Application to liquid water. *Faraday Discuss.* **1978**, *66*, 58–70.

(36) Van der Zwan, G.; Hynes, J. T. Dynamical Polar Solvent Effects on Solution Reactions: A Simple Continuum Model. *J. Chem. Phys.* **1982**, *76*, 2993–3001.

(37) Van der Zwan, G.; Hynes, J. T. Time-Dependent Fluorescence Solvent Shifts, Dielectric Friction, and Nonequilibrium Solvation in Polar Solvents. *J. Phys. Chem.* **1985**, *89*, 4181–4188.

(38) Pipolo, S.; Corni, S.; Cammi, R. The Cavity Electromagnetic Field within the Polarizable Continuum Model of Solvation. *J. Chem. Phys.* **2014**, *140*, 164114–30.

(39) Chernyak, V.; Mukamel, S. Density-Matrix Representation of Nonadiabatic Couplings in Time-Dependent Density Functional (TDDFT) Theories. *J. Chem. Phys.* **2000**, *112*, 3572–3579.

(40) Chernyak, V.; Mukamel, S. Time-Dependent Density-Matrix Functional in Liouville Space and the Optical Response of Many-Electron Systems. *Phys. Rev. A* **1995**, *52*, 3601–3621.

(41) Isborn, C. M.; Li, X.; Tully, J. C. Time-Dependent Density Functional Theory Ehrenfest Dynamics: Collisions Between Atomic Oxygen and Graphite Clusters. *J. Chem. Phys.* **2007**, *126*, 134307–134307.

(42) Cheng, C.; Evans, J. S.; Van Voorhis, T. Simulating Molecular Conductance Using Real-Time Density Functional Theory. *Phys. Rev. B* **2006**, *74*, 155112–155123.

(43) Magnus, W. On the Exponential Solution of Differential Equations for a Linear Operator. *Comm. Pure Appl. Math.* **1954**, *7*, 649–673.

(44) Blanes, S.; Casas, F.; Ros, J. Improved High Order Integrators Based on the Magnus Expansion. *BIT Num. Math.* **2000**, *40*, 434–450.

(45) Li, X.; Smith, S. M.; Markevitch, A. N.; Romanov, D. A.; Levis, R. J.; Schlegel, H. B. A Time-Dependent Hartree-Fock Approach for Studying the Electronic Optical Response of Molecules in Intense Fields. *PCCP* **2005**, *7*, 233–239.

(46) Atkinson, K. E. *An Introduction to Numerical Analysis*; John Wiley & Sons, 2008.

(47) Becke, A. D. Density-Functional Exchange-Energy Approximation with Correct Asymptotic Behavior. *Phys. Rev. A* **1988**, *38*, 3098–3100.

(48) Dunning Jr, T. H. Gaussian Basis Sets for Use in Correlated Molecular Calculations. I. The Atoms Boron Through Neon and Hydrogen. *J. Chem. Phys.* **1989**, *90*, 1007–1023.

(49) Press, W. H. *Numerical Recipes 3rd Edition: The Art of Scientific Computing*; Cambridge university press, 2007.

(50) Frisch, M. J.; Trucks, G. W.; Schlegel, H. B.; Scuseria, G. E.; Robb, M. A.; Cheeseman, J. R.; Scalmani, G.; Barone, V.; Mennucci, B.; Petersson, G. A.; *et al.*, Gaussian 09. 2009; Gaussian Inc. Wallingford CT.

(51) Cossi, M.; Scalmani, G.; Rega, N.; Barone, V. New Developments in the Polarizable Continuum Model for Quantum Mechanical and Classical Calculations on Molecules in Solution. *J. Chem. Phys.* **2002**, *117*, 43–54.

(52) Kong, Y.; Ponder, J. W. Calculation of the Reaction Field Due to Off-Center Point Multipoles. *J. Chem. Phys.* **1997**, *107*, 481–492.

(53) Fuchs, R. Theory of the Optical Properties of Ionic Crystal Cubes. *Phys. Rev. B* **1975**, *11*, 1732–1740.

(54) Hohenester, U.; Trugler, a. Interaction of Single Molecules With Metallic Nanoparticles. *IEEE J. Sel. Top. Quant.* **2008**, *14*, 1430–1440.

Graphical TOC Entry